

Newly proposed quantitative criteria can assess chronic atrophic gastritis via probe-based confocal laser endomicroscopy (pCLE): a pilot study



Authors

Carlos Robles-Medranda, Miguel Puga-Tejada, Roberto Oleas, Jorge Baquerizo-Burgos, Juan Alcívar-Vásquez, Raquel Del Valle, Carlos Cifuentes-Gordillo, Haydee Alvarado-Escobar, Daniel Ponce-Velez, Jesenia Ospina-Arboleda, Hannah Pitanga-Lukashok

Institution

Gastroenterology and Endoscopy Division, Instituto Ecuatoriano de Enfermedades Digestivas (IECED), Guayaquil, Ecuador

submitted 15.12.2020

accepted after revision 16.8.2021

Bibliography

Endosc Int Open 2022; 10: E297–E306

DOI 10.1055/a-1662-5150

ISSN 2364-3722

© 2022. The Author(s).

This is an open access article published by Thieme under the terms of the Creative Commons Attribution-NonDerivative-NonCommercial License, permitting copying and reproduction so long as the original work is given appropriate credit. Contents may not be used for commercial purposes, or adapted, remixed, transformed or built upon. (<https://creativecommons.org/licenses/by-nc-nd/4.0/>)

Georg Thieme Verlag KG, Rüdigerstraße 14, 70469 Stuttgart, Germany

Corresponding author

Carlos Robles-Medranda, MD, Head of the Endoscopy Division, Instituto Ecuatoriano de Enfermedades Digestivas – IECED, Av. Abel Romeo Castillo & Av. Juan Tanca Marengo, Torre Vitalis, Mezzanine 1, Guayaquil, Ecuador
Fax: +59342109180
carlosoakm@yahoo.es

ABSTRACT

Background and study aims Probe-based confocal laser endomicroscopy (pCLE) can provide high magnification to evaluate chronic atrophic gastritis (CAG), but the current pCLE criteria are qualitative and prone to variability. We aimed to propose a quantitative CAG criterion based on pCLE to distinguish non-atrophic gastritis (NAG) from CAG. **Patients and methods** This observational, exploratory pilot study included patients with NAG and CAG evaluated via esophagogastroduodenoscopy, pCLE, and histology. We measured the gastric glands density, gastric gland area, and inter-glandular distance during pCLE.

Results Thirty-nine patients (30/39 with CAG) were included. In total, 194 glands were measured by pCLE, and 18301 were measured by histology, with a median of five glands per NAG patient and 4.5 per CAG patient; pCLE moderately correlate with histology ($\rho=0.307$; $P=0.087$). A gland area of 1890–9105 μm^2 and an inter-glandular distance of 12 to 72 μm based on the values observed in the NAG patients were considered normal. The proposed pCLE-based CAG criteria were as follows: a) glands density <5 ; b) gland area $<1/16$ the pCLE field area ($<1890 \mu\text{m}^2$) or $>1/4$ the pCLE field area ($>9105 \mu\text{m}^2$); or c) inter-glandular distance <12 or $>72 \mu\text{m}$; CAG was diagnosed by the presence of at least one criterion. The proposed criteria discriminated CAG with a ranged sensitivity of 76.9% to 92.3%, a negative predictive value of 66.6% to 80.0%, and 69.6% to 73.9% accuracy.

Conclusions The proposed pCLE criteria offer an accurate quantitative measurement of CAG with high sensitivity and excellent interobserver agreement. Larger studies are needed to validate the proposed criteria.

Introduction

Chronic atrophic gastritis (CAG) represents an early stage in gastric cancer's pathogenesis [1]. Endoscopy-based epidemiological studies show that CAG has a prevalence of $<50\%$ (2); how-

ever, recent data from Japan and China showed higher rates [2]. A Swedish population-based cohort study showed a 2.8 (95% CI 2.3 to 3.3) standardized incidence of gastric cancer in CAG patients, higher in comparison to the 1.8 (95% CI 1.7 to 1.9) incidence in non-atrophic gastritis (NAG) patients [3].

Improvements in CAG diagnosis may identify patients at risk for gastric cancer while still in the early stages of CAG, thus avoiding more invasive or unnecessary oncological treatment [4]. Routinely, histological evaluation of endoscopic biopsies is considered the gold standard for evaluating gastrointestinal tract lesions [5]. However, histological assessment of CAG based on these biopsies is susceptible to a sampling error as high as 20–30%, interpretation mistakes, inadequate biopsy forceps sampling sites, and insufficient numbers of acquired biopsies [5]. Additionally, CAG histological diagnosis has low concordance with CAG diagnosis based on endoscopic visualization alone, especially in the gastric body [6], leading to further potential for misinterpretation.

To reduce the histological misclassification, the updated Sydney system, established in Houston in 1994, proposed that CAG be graded as mild, moderate, or severe, using a visual analog scale [7]. The severity of atrophic gastritis is based on the gradual loss and subsequently decreased density of gastric glands [8], which are associated with chronicity features such as an increased inter-glandular distance, foveolar hyperplasia [9], and intestinal metaplasia [10]. However, this system produces only a moderate interobserver agreement, mainly due to the visual analog scale limitations [11, 12]. To date, histological assessments of CAG have not considered the gland size or inter-glandular distance [13, 14], as histological evaluation of these features requires appropriate specimen sections.

High-definition endoscopy with narrow-band imaging (NBI) has shown good sensitivity and specificity for detecting gastric precancerous lesions. However, there is a lack of agreement about whether the NBI pattern is associated with gastric precancerous lesions [1]. An observational study found higher accuracy of probe-based confocal laser endomicroscopy (pCLE) for detecting CAG (84.7%) compared to chromoendoscopy (81.74%) and NBI (79.84%) [15]. pCLE is an optical biopsy method that offers *in vivo* microscopic imaging of the gastrointestinal mucosa at 1000-fold magnification, enabling high diagnostic accuracy and a positive impact on gastrointestinal tract lesions management [16]. The CAG features as evaluated via pCLE have been qualitatively described [17]; however, a quantitative description might provide more reproducible results.

Based on the knowledge that CAG severity affects gastric glands density, gland size, and inter-glandular distance, we aimed to quantitatively assess the severity of CAG by measuring the abovementioned features in patients with NAG and CAG via pCLE and propose novel quantitative criteria for evaluating CAG with pCLE.

Patients and methods

Study design

This was an observational, descriptive, prospective exploratory pilot study conducted at a tertiary center in Ecuador. The study was organized into two phases: 1) Development of the pCLE criteria for CAG, and 2) Validation of the proposed criteria. The study protocol was reviewed and approved by the Institutional Ethics Committee and registered on ClinicalTrials.gov under the

code NCT02351154. The study was conducted in accordance with the Declaration of Helsinki and following the CONSORT 2010 extension for pilot studies guidelines [18]. All enrolled patients provided written informed consent before the endoscopic procedures.

Phase I: Development of the pCLE criteria for CAG

Patient selection

We prospectively enrolled patients aged ≥ 18 years with a recent histological diagnosis of CAG or NAG in accordance with the updated Sydney classification system (2 weeks after histological confirmation) between September 2014 and March 2015. Before enrollment, the patients complained of ulcer-like type dyspepsia for ≥ 12 months. We excluded patients who were on proton pump inhibitor (PPI) therapy, were pregnant or nursing, were taking nonsteroidal anti-inflammatory drugs (NSAIDs) or antibiotics two weeks before enrollment, had a personal history of surgery to treat gastric cancer, had received *H. pylori* eradication therapy in the past, or had a known allergy history to fluorescein.

Endoscopic procedure

All participants underwent esophagogastroduodenoscopy with white-light examination using a high-definition endoscope (Pentax EG-2990-i; Pentax Medical Co, Japan). Endoscopic procedures were performed with the patient in the left lateral decubitus position under conscious sedation with an intravenous propofol infusion and continuous vital sign monitoring. Endoscopy and forceps biopsy sampling was performed in accordance with the updated Sydney system guidelines [7].

pCLE evaluation

During esophagogastroduodenoscopy, an endomicroscopic evaluation of the gastric body mucosa performed using the GastroFlex probe (Cellvizio, Mauna Kea Technology, Paris, France) through the accessory channel of the scope. We defined the region of interest for pCLE evaluation based on the diagnosis impression during high-definition white-light endoscopy. The probe was gently placed in contact with the mucosa to avoid trauma. Before the pCLE evaluation, 5 mL of 10% fluorescein (BioGlo, Sofar Productos, Bogota, Colombia) was intravenously injected immediately before pCLE evaluation. We considered only the gastric body mucosa because these glands are smaller compared to those in the antrum, allowing a convenient analysis in the 240- μm -diameter pCLE field.

The pCLE images were recorded as video-frames and images for postprocedural analysis with Cellvizio Viewer (CV) software, which offers micrometric (μm) measurement of observed structures during pCLE evaluation.

Esophagogastroduodenoscopy and endomicroscopic evaluations were performed by one endoscopist (C.R.-M.), who had performed 80 pCLE evaluations before the patient's enrollment. Proficiency in pCLE was defined as completion of training and certification by the manufactures of pCLE. The operator was blinded to the patients' medical records. The pCLE evalua-

tion of the gastric glands was performed following the criteria proposed by Zhang et al. [17].

Based on the rationale that gastric glands are elliptical, we calculated the gland area (A) using CV software as follows:

$$A(\mu\text{m}^2) = \pi \times \frac{\text{larger diameter}}{2} (\mu\text{m}) \times \frac{\text{shorter diameter}}{2} (\mu\text{m})$$

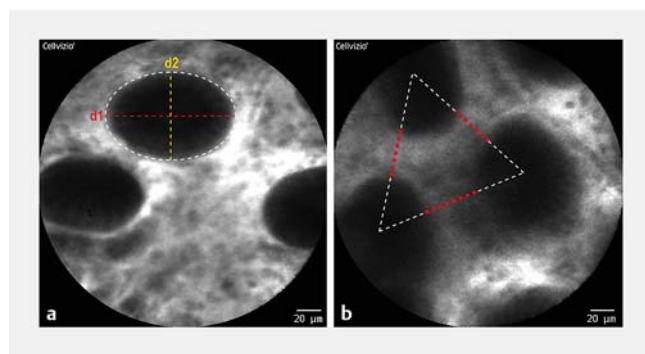
The larger and shorter diameter of the ellipse corresponded to the major (d1) and the minor axis (d2); they are represented in ►Fig.1a as a red and yellow line for illustrative purposes, respectively.

The inter-glandular distance was defined as the space between adjacent gland borders, as measured between the corresponding gland centers. ►Fig. 1b shows inter-glandular distance measurements with white and red lines, for illustrative purposes. The white lines represent the pathways between the centers of the adjacent glands used to measure inter-glandular distance. Red lines represent the measured inter-glandular distances per se.

Histological evaluation

After pCLE evaluation, forceps biopsies were obtained from the same area evaluated via pCLE. Two samples were taken from the lesser and greater curvatures of the antrum approximately 2 to 3 cm from the pylorus. Two were taken from the middle portion of the lesser and greater curvatures of the body about 8 cm from the cardia, and one biopsy was taken from the angulus.

For histological analysis, the specimens were fixed in 10% formalin after tissue acquisition, embedded in paraffin for sectioning, and stained with hematoxylin and eosin (H&E). An experienced gastrointestinal pathologist blinded to the medical records and endoscopic findings evaluated the specimens using a Nikon white-light microscope (Nikon Instruments Inc., New York, New York, United States). The histological grading of CAG was performed following the updated Sydney classification system [3]. Specimens with fewer than 20 glands on histological examination were excluded from the analysis to avoid misinterpretations [10].



► **Fig. 1** Gastric gland measurements via pCLE. **a** Diameter measurements: major axis (d1, red line) and minor axis (d2, yellow line). **b** Gastric inter-glandular distance measurements: white lines represent the pathways between the centers of the adjacent glands used to measure inter-glandular distance, and the red lines represent the measured inter-glandular distances.

The specimens from the gastric body were observed on 10X photomicrographs in Tagged Image File Format (.tiff) files and quantitatively assessed by the same gastrointestinal pathologist, who counted the total number of glands for each specimen using NIS-elements D v4.6 imaging software (Nikon Instruments Inc., New York, USA).

Statistical analysis

Technical considerations

The data analysis was performed by two institutional biostatisticians (M.P.-T. and J.O.-A.) using R v3.6.3 (R Foundation for Statistical Computing, Vienna, Austria). $P < 0.05$ was considered statistically significant, and between 0.05–0.10 moderately significant.

Sample size

A sample of 21 cases was calculated to be appropriate for the study purposes. We used a two-sided formula for estimating the number of subjects required for a study of interobserver agreement with a binary outcome, processed through the R library “kappaSize” [19]. We based on the CAG agreement (kappa=0.531) from gastric body biopsies [11]. It was considered two raters; an alpha and beta error of 5% and 20%, respectively; a kappa=0.2 as slight agreement (null hypothesis), and a kappa=0.8 as excellent agreement (alternative hypothesis).

Baseline characteristics

Quantitative variables are described as the median (minimum–maximum range) or mean (standard deviation, SD) according to their statistical distribution. Qualitative variables are described as frequency (%). Demographic data, pCLE, and histological findings were described and compared between the NAG and CAG cohorts using Student’s *t* or Mann-Whitney U test for quantitative variables and Fisher’s exact or Pearson’s chi-squared test for qualitative variables.

Correlation of pCLE-based and histology-based glands density

The number of observed glands for each patient was correlated between pCLE and histology using Spearman’s rank correlation coefficient (rho). Gland density on pCLE and histology for patients with NAG and CAG were estimated by the median number of glands and compared using the corresponding hypothesis tests.

pCLE morphometric gland analysis

The normal ranges for gland size, inter-glandular distance, and gland density were determined based on the observed minimum–maximum range for each parameter in the NAG patients, and each pCLE glands were respectively classified as NAG or CAG according to these average values. In determining this normal range, gland diameter (D) was calculated as follows:

$$D(\mu\text{m}) = \sqrt{\frac{\text{atrophy - on - going cut - off area } (\mu\text{m}^2)}{\pi}} \times 2$$

This method presents an optical and indirect manner to measure the normal gland area in comparison to that of a 240- μm -diameter pCLE field.

We performed a circle-packing analysis using an online calculator to define the hypothetical number of glands that could completely fit within a pCLE field (https://www.engineering-toolbox.com/smaller-circles-in-larger-circle-d_1849.html).

The inter-glandular distance on pCLE was described within the inter-glandular distance range determined in the NAG cohort.

Phase II: Validation of pCLE-CAG proposed criteria

A set of 23 pCLE videos from different cases than the original cohort of patients were arbitrary selected from the enrolled patient by the operating endoscopist (C.R.-M.). Four expert endoscopists (J.A.-V., R.V.-Z., C.C.-G. and H.A.-E) and non-expert physicians (R.O., J.B.-B., J.O.-A and H.P.-L) who were blinded to the endoscopic and histological findings performed an off-line evaluation as part of the pCLE-CAG criteria validation. The diagnoses were given using the proposed pCLE criteria for CAG, as explained below. Additionally, endoscopists evaluated the same pCLE videos seven days later for the intra-observer evaluation. All pCLE sequences were displayed in their original image format (.mkt, Mauna Kea Technologies, Paris, France).

Overall accuracy

The pCLE-CAG proposed criteria for overall accuracy were evaluated in terms of sensitivity, specificity, positive and negative predictive value (PPV and NPV, respectively), positive and negative likelihood ratios, and accuracy. CAG versus NAG classification determined by the proposed pCLE criteria was compared with CAG versus NAG classification as determined by the initial histological type in calculating these statistics.

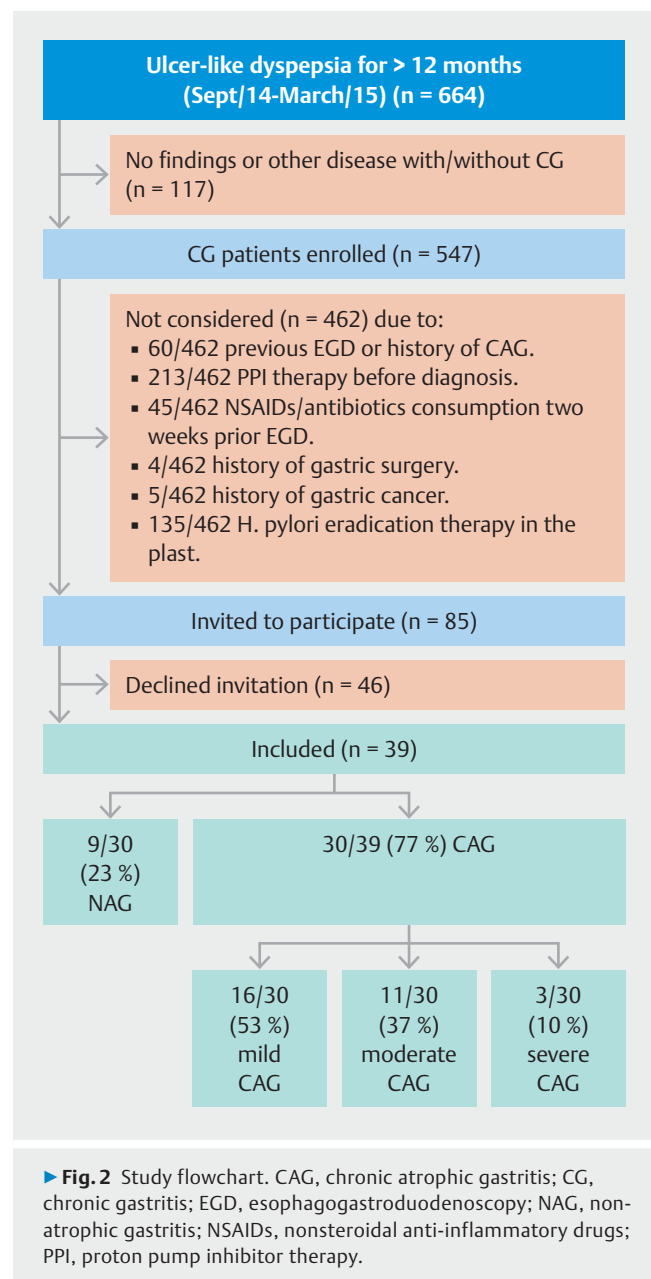
Interobserver and intra-observer agreement

Additionally, Interobserver and intra-observer agreement was estimated for each endoscopist through Cohen's kappa and Fleiss' kappa coefficients and interpreted according to the criteria of Landis and Koch.

Results

Baseline characteristics

We included 39 patients with a median age of 42 years (24–85); 21 of 39 (53.8%) were female. According to pCLE, intra-gland fluorescein leakage was presented in five of 31 cases (12.8%), respectively. According to histology, chronic active gastritis and *Helicobacter pylori* infection were present in three of 39 (7.7%) and six of 39 cases (15.4%), respectively. We included nine of 39 patients (23.1%) with NAG and 30 of 39 (76.9%) with CAG: 16 of 30 with mild CAG, 11 of 30 with moderate CAG, and three of 30 with severe CAG (► Fig. 2). There were no significant differences in demographic, pCLE, or histopathological characteristics between the NAG and CAG patients (► Table 1).



Glands density on pCLE and histology

We evaluated 194 glands via pCLE (49 in the NAG cohort and 145 in the CAG cohort) and 18301 glands histologically (5705 in the NAG cohort and 12596 in the CAG cohort) in all included patients. The median number of glands per patient was five (range: 1–22) and 538 (range: 47–1255), respectively. The number of observed glands was directly correlated between pCLE and biopsy ($\rho=0.307$; 95% CI 0.047–0.592; $P=0.087$), explaining the reduction in glands number atrophic gastritis pathogeny was similarly estimated both by pCLE and biopsy analysis. The median total number of glands was higher in the NAG cohort than in the CAG cohort via pCLE (5 versus 4.5; $P=0.2431$) and histology (800 vs. 416; $P=0.0270$). Furthermore, there was a median of two and 145 glands measured via pCLE

► **Table 1** Baseline characteristics of the patients enrolled in the study.

	Total (n=39)	NAG cohort (n=9)	CAG cohort (n=30)	P value
Demographic data				
Age (years), median (range)	42 (24–85)	38 (29–64)	44.5 (24–85)	0.1713 ¹
Sex (female), n (%)	21 (53.8)	4 (44.4)	17 (56.7)	0.7062 ²
Histopathological diagnosis				
CAG grade (Sydney), n (%)				–
Mild CAG	16 (41.0)	–	16 (53.3)	
Moderate CAG	11 (28.2)	–	11 (36.7)	
Severe CAG	3 (7.7)	–	3 (10.0)	
Chronic active gastritis, n (%)	3 (7.7)	1 (11.1)	2 (6.7)	0.5558 ²
<i>H. pylori</i> infection, n (%)	6 (15.4)	3 (33.3)	3 (10.0)	0.1225 ^{1,2}
CAG, chronic atrophic gastritis; NAG, non-atrophic gastritis; pCLE, probe-based confocal laser endomicroscopy.				
¹ Mann-Whitney U test.				
² Fisher's exact test for count data.				

and histology, respectively, in severe CAG cases (► **Table 2**), showing that glands density was correlated with CAG severity.

pCLE morphometric gland analysis

Gland area

The 49 of 194 glands (25.3%) evaluated by pCLE from the NAG cohort had a median gland area of 4460 μm^2 (range: 1890–9105 μm^2). After confirming the normal distribution of the gland area values in the NAG and CAG cohorts via the Jarque-Bera test ($P=0.2016$), we also observed that the gland area in the NAG cohort was smaller than that in the CAG cohort (4460 vs. 4280 μm^2 , $P=0.7595$).

The NAG gland area observed was used to define the normal range and was applied to glands analysis in the CAG cohort. Among the 145 of 194 glands (74.7%) from the CAG cohort, 13 of 145 glands (9%) had an area smaller than 1890 μm^2 , and nine of 145 glands (6.2%) were larger than 9105 μm^2 ($p=0.0151$). Among the smaller glands, seven of 13 and six of 13 corresponded to mild CAG and moderate CAG; among the larger glands, two of nine, five of nine, and two of nine corresponded to mild CAG, moderate CAG, and severe CAG, respectively ($P=0.0045$) (► **Table 2**, ► **Fig. 3a**). The gland areas of 1890 and 9105 μm^2 correspond to gland diameters of 50 and 108 μm , respectively. According to the circle packing analysis, 16 50- μm -diameter or three 108- μm -diameter glands could be packed in a 240- μm -diameter region. Considering that the 240- μm -diameter pCLE field is a circle, and this circle could be theoretically divided into four equal quadrants, and each quadrant in another four equal quadrants (1/16); a gland larger than one-quarter of the pCLE field is optically larger than a 108- μm -diameter gland; and a gland with an area smaller than one-sixteenth of the pCLE field is optically smaller than a 50- μm -diameter (► **Fig. 4a**, ► **Fig. 4b**).

Inter-glandular distance

A total of 194 inter-glandular distances were measured (49 in the NAG cohort and 145 in the CAG cohort). In the NAG cohort, the inter-glandular distance ranged from 12 to 72 μm . The NAG cohort's pCLE inter-glandular distance measurements were normally distributed, as shown by a nonsignificant Jarque-Bera test ($P=0.1185$). We observed a nonsignificant increase in inter-glandular distance between the NAG and CAG cohorts (32.5 vs. 38 μm , respectively). Applying the observed range of NAG inter-glandular distances as the typical values, there were 12 of 145 (8.3%) and five of 145 (3.4%) inter-glandular distances in the CAG cohort that were shorter than 12 μm and longer than 72 μm ($P=0.0429$), respectively. Of the inter-glandular distances shorter than 12 μm , six of 12, five of 12, and one of 12 corresponded to mild, moderate and severe CAG cases; of the inter-glandular distances longer than 72 μm , the three measurements each corresponded to mild, moderate and severe CAG ($P=0.0738$) (► **Table 2**). As shown in ► **Fig. 3b**, four of 12 inter-glandular distances shorter than 12 μm were measured as 0 μm , recalling the back-to-back gland placement.

Proposed pCLE-based criteria for CAG

Based on the morphometric analysis and the number of glands evaluated by pCLE, two endoscopists (C.R.-M. & H.P.-L.), one biostatistician (M.P.-T.) and a gastrointestinal pathologist assessed the pCLE videos of the enrolled patients and the results of the pCLE gland analysis (► **Fig. 3**) to propose pCLE criteria for defining CAG.

We proposed three pCLE criteria with the presence of at least one criterion defining CAG: a) a density of less than five glands per patient; b) the presence of a gland smaller than one of 16 of the pCLE field circumference (<1890 μm^2) (► **Fig. 4a**) or the presence of a gland larger than one-quarter of the pCLE field circumference (>9105 μm^2) (► **Fig. 4b**); or c) an inter-glandular distance <12 or >72 μm (► **Fig. 4c**).

Table 2 Histology and pCLE morphometric analysis: gland area (μm^2) and inter-gland distance (μm) of the NAG and CAG cohorts.

	NAG (n=9)	CAG (n=30)	P value	CAG grades			P value
				Mild (n=16)	Moderate (n=11)	Severe (n=3)	
Histology							
No. of glands	5705	12596	–	5552	5749	1295	–
Median (range)	800 (538–1100)	416 (47–1260)	0.0270 ¹	414 (47–1160)	508 (155–1260)	145 (131–1020)	0.1005 ²
pCLE							
No. of glands	49	145	–	67	71	7	–
Median (range)	5 (2–10)	4.5 (1–22)	0.2431 ¹	5 (2–8)	5 (2–22)	2 (1–4)	0.1209 ²
Gland area (μm^2), median (range)	4460 (1890–9100)	4280 (848–19000)	0.7595 ¹	4170 (1080–19000)	4260 (848–14800)	6380 (5170–13500)	0.0210 ²
<1890 μm^2	–	13 (9.0)	0.0151 ³	7 (10.4)	6 (8.5)	–	0.0045 ³
1890–9100 μm^2	49 (100%)	123 (84.8)		58 (86.6)	60 (84.5)	5 (71.4)	
>9100 μm^2	–	9 (6.2)		2 (3.0)	5 (7.0)	2 (28.6)	
Inter-glandular distance (μm), median (range)	32.5 (12.0–71.9)	38.0 (0–81.9)	0.6631 ¹	35.7 (0–75.6)	39.0 (0–81.9)	29.0 (0–81.0)	0.3724 ²
<12 μm	–	12 (8.3)	0.0429 ¹	6 (9.0)	5 (7.0)	1 (14.3)	0.0738 ³
12–72 μm	49 (100.0)	128 (88.3)		60 (89.6)	63 (88.7)	5 (71.4)	
>72 μm	–	5 (3.4)		1 (1.5)	1 (1.4)	1 (14.3)	

CAG, chronic atrophic gastritis; NAG, non-atrophic gastritis; pCLE, probe-based, confocal laser endomicroscopy.

¹ Wilcoxon rank sum test with continuity correction.

² Kruskal-Wallis rank sum test.

³ Pearson's chi-squared test.

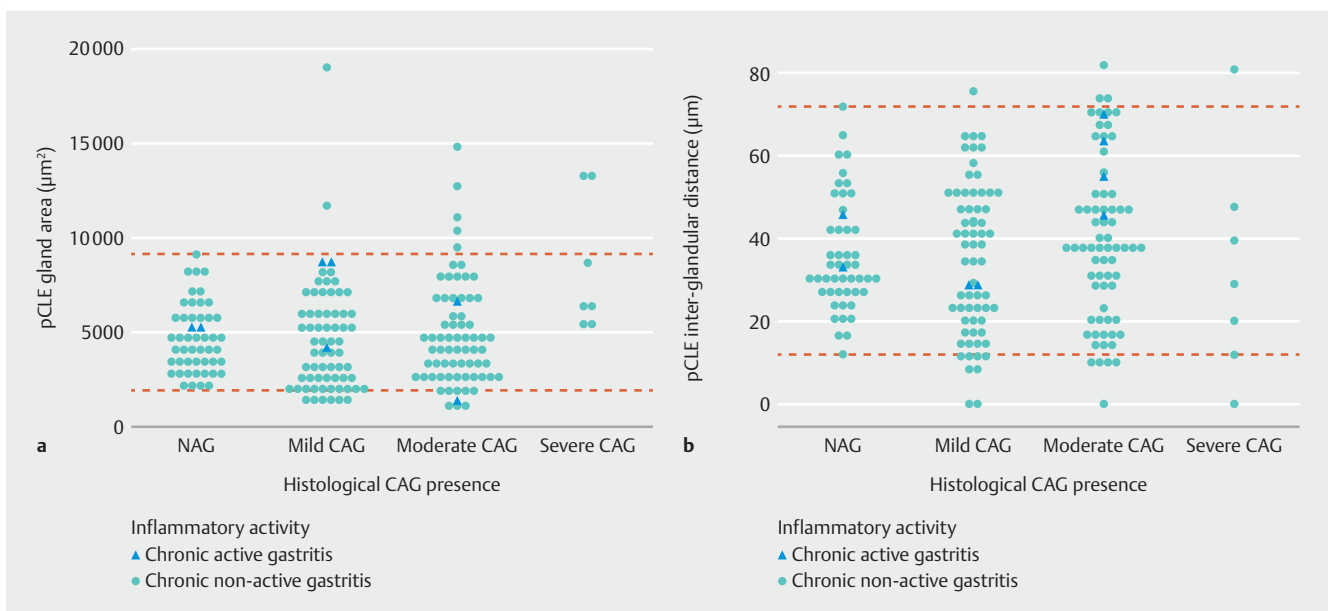
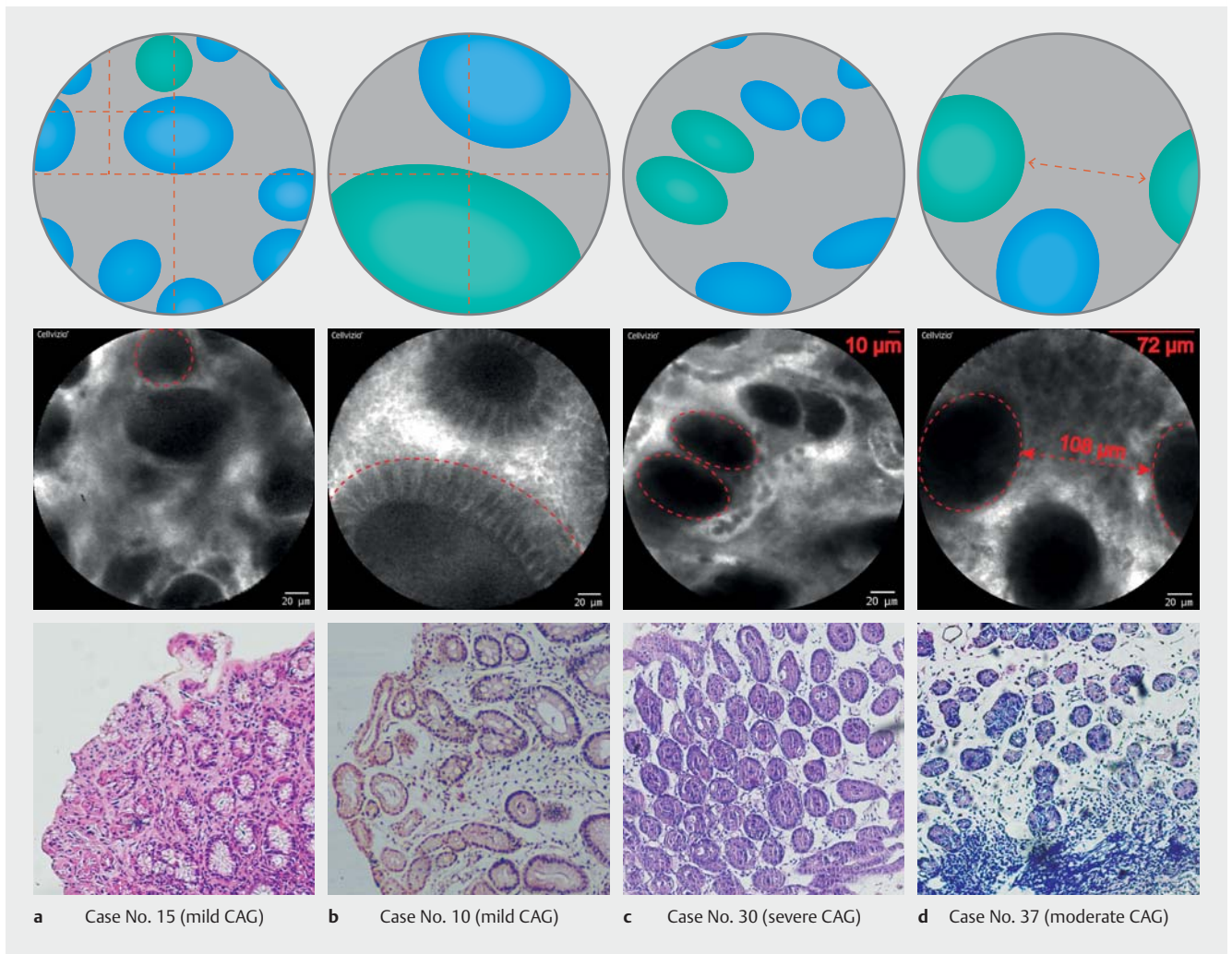


Fig. 3 Boxplots describing the: **a** statistical distribution of pCLE gastric gland area and **b** inter-glandular distance in non-atrophic and chronic atrophic gastritis (NAG and CAG, respectively). Each yellow circle represents a gastric gland with non-active chronic gastritis. Each blue triangle represents a gastric gland with active chronic gastritis. The dashed red lines indicate the minimum and maximum measurements in the NAG cohort.



► **Fig. 4** Schematic representation of pCLE criteria for chronic atrophic gastritis (CAG) based on quantitative measurements during pCLE. **a** Presence of a gland smaller than 1/16 pCLE field ($<1890 \mu\text{m}^2$). **b** Presence of a gland larger than 1/4 pCLE field ($>9105 \mu\text{m}^2$). **c** Presence of a short inter-glandular distance (<12 or $>72 \mu\text{m}$).

Overall accuracy

We estimated that the above criteria had the highest sensitivity, specificity, PPV, NPV, and accuracy of 92.3%, 60.0%, 71.4%, 83.3%, and 73.9%, respectively, for defining CAG via pCLE when applied by expert endoscopists. ► **Table 3** details the overall accuracy of pCLE criterion for each endoscopists included in the study. These results showed that these criteria reached an excellent sensitivity, PPV, NPV, and accuracy, but low specificity.

Interobserver and intra-observer agreement

The interobserver and intra-observer agreement rates between expert endoscopists and non-expert physicians for each pCLE criteria are summarized on ► **Table 4**. These results showed that with these criteria, experts and non-experts could classify analyzed cases between NAG versus CAG with a moderate interobserver and excellent intra-observer agreement.

Discussion

Currently, there is a lack of a universal consensus regarding classification systems to distinguish CAG and NAG, with the available system being based on a qualitative analog scale that limits its reproducibility and agreement between observers; accordingly, there is a high risk of variability during diagnostic interpretation [20]. A successful classification system based on histology, endoscopy, or pCLE should accurately characterize CAG with high reproducibility [21]. In the present study, we evaluated CAG identification via pCLE based on gastric gland density, gland area, and inter-glandular distance measurements. We proposed these three quantitative criteria for diagnosing CAG.

First, we confirmed that gastric gland density is directly correlated with CAG severity in both pCLE and histological evaluations. This finding agrees with previous histological morphometric studies [8, 13, 14]. Second, we found that compared to NAG, CAG patients had larger and smaller gland areas meas-

Table 3 Overall accuracy of proposed pCLE criteria for histological confirmed chronic atrophic gastritis (CAG) implemented by four endoscopists.

	J. A-V.	R. V-Z.	C. C-G.	H. A-E.
Sensitivity	12/13; 92.3% (63.9–99.9)	12/13; 92.3% (64.0–99.8)	12/13; 92.3% (63.9–99.9)	10/13; 76.9% (46.2–95.0)
Specificity	4/10; 40.0% (12.2–73.8)	5/10; 50.0% (18.7–81.3)	4/10; 40.0% (12.2–73.8)	6/10; 60% (26.2–87.8)
PPV	12/18; 66.7% (40.9–86.7)	12/17; 70.6% (44.0–89.7)	12/18; 66.7% (40.9–86.7)	10/14; 71.4% (41.9–91.6)
NPV	4/5; 80.0% (28.4–99.5)	5/6; 83.3% (35.9–99.6)	4/5; 80.0% (28.4–99.5)	6/9; 66.6% (29.9–92.5)
PLR	1.54 (0.91–2.61)	1.85 (0.97–3.50)	1.54 (0.91–2.61)	1.92 (0.85–4.35)
NLR	0.19 (0.03–1.46)	0.15 (0.02–1.11)	0.19 (0.03–1.46)	0.38 (0.13–1.17)
Accuracy	16/23; 69.6% (47.1–86.8)	17/23; 73.9% (51.6–89.8)	16/23; 69.6% (47.1–86.8)	16/23; 69.6% (47.1–86.8)

NLR, negative likelihood ratio; NPV, negative predictive value; pCLE, probe-based confocal laser endomicroscopy; PLR, positive likelihood ratio; PPV, positive predictive value.

ured on pCLE; this variation correlated with CAG grade. Larger glands may be interpreted due to foveolar hyperplasia, a proliferation, elongation, and tortuosity of gastric glands as a compensatory response to chronic inflammation of the gastric mucosa [22]. Smaller glands may be interpreted as areas undergoing atrophy. Third, in the CAG cohort, we found that some glands appeared to be nearly adjacent, similar to the back-to-back glandular placement observed in gastric dysplasia by hematoxylin and eosin histopathological staining [22]. It is important to note that the pCLE gastric dysplasia criteria include crowded glands with variable degrees of intraluminal folding, but not glands with a back-to-back organization [23].

Based on these findings, we proposed three quantitative criteria based on gland density, gland area, and inter-glandular distance to diagnose CAG. Our proposed pCLE criteria implemented by four expert endoscopists reached a high sensitivity (92.3%), PPV (71.4%), NPV (83.3%), and accuracy (73.9%) for detecting CAG. Also, an excellent agreement between observers when they used the proposed pCLE criteria to define CAG. Several studies have also assessed the capacity of pCLE for detecting CAG. In 2008, CAG via pCLE was defined as "the number of glands decreasing and/or prominently dilating." These qualitative criteria predicted atrophic gastritis with a sensitivity, specificity, PPV, and NPV of 83.6%, 99.6%, 96.6%, and 97.6%, respectively [17]. In 2010, a similar CAG definition via pCLE reached a sensitivity, specificity, PPV, and NPV of 92.9%, 95.2%, 72.5%, and 98.9%, respectively [24]. Our proposed pCLE criteria for CAG reached a higher sensitivity and NPV through a quantitative way.

A pooled analysis from five Ecuadorian studies between 2013 and 2018 estimated a 1-year endoscopy-based CAG incidence of 38.1% (95% CI 28.5–49.0) [25], as in other Western countries (lower than 50%) [2]. Recent studies on CAG detection via pCLE are from Chinese populations [15, 17, 24, 26],

where CAG prevalence is much higher than in Western countries. Pathologists are familiar with the specific types of prevalent gastritis where they practice. CAG description could be difficult due to epidemiological circumstances [14].

Recently, a new quantitative method to characterize CAG via pCLE has been published. It concluded that a gastric inter-glandular distance $>30\mu\text{m}$ detects CAG with a sensitivity and specificity of 85.7% and 93.8%, respectively [26]. Although this study used the rationale that increased inter-glandular distance is associated with atrophy, it lacked a detailed definition of how inter-glandular distance was measured. In contrast, our study is the first to objectively describe inter-glandular distance measurement, useful when reproducing it as a pCLE criterion for CAG in clinical practice. Moreover, it was observed a significantly increased vessel diameter in patients with CAG compared to controls. Increased vessel diameter has also been associated with inflammation in chronic diseases [27]. Inflammation could be considered an indicator of gastritis activity, as it is a recognized factor that makes histological assessments of CAG challenging [13]. Although we did not consider pCLE or histopathological inflammatory activity criteria as exclusion criteria from this pilot study, five of 39 cases (12.8%) presented intra-glandular fluorescein leakage at pCLE three of 39 (7.7%) showed chronic active gastritis at biopsy, with no significant difference between CAG and NAG cohorts.

The previously cited research also evaluated gland density. Like the current study, it has been observed that the mean number of gastric glands in glandular atrophy was significantly lower than that in controls (20 vs. 5 glands per patient; $P \leq 0.001$) [24]. Nevertheless, previous studies did not clarify whether a standardized area of interest (AOI) was considered. A mean of five versus two to three glands per patient when comparing controls versus CAG cases has been described, but without a predefined AOI to obtain this measurement [26]. The

► Table 4 Interobserver and intra-observer analysis of the proposed pCLE criteria for CAG (Cohen's Kappa value [P value]) between expert and non-expert endoscopists.

	Density <5 glands per patient	Gland's area		Inter-glandular distance		
		Presence of a gland as small as 1/15 pCLE field circumference (<1890 μm^2)	Presence of a gland as large as 1/4 pCLE field circumference (>9105 μm^2)	Presence of a close inter-glandular distance (<12 μm)	Presence of a far inter-glandular distance (>72 μm)	
Expert endoscopists						
Inter-OA	0.646 (<0.001)	0.418 (<0.001)	0.228 (0.0073)	0.285 (0.0008)	0.471 (<0.001)	
Intra-OA	JMA	0.911 (<0.001)	0.620 (0.0024)	0.738 (0.0004)	0.832 (<0.001)	0.823 (<0.001)
	RVZ	0.649 (0.0016)	0.069 (0.6920)	0.496 (0.0157)	0.511 (0.0050)	0.881 (<0.001)
	CCG	0.534 (0.0100)	0.469 (0.0244)	0.679 (0.0011)	0.452 (0.0300)	0.563 (0.0068)
	HAE	0.810 (<0.001)	0.389 (0.0565)	0.563 (0.0068)	0.657 (0.0008)	0.679 (0.0011)
Non-expert physicians						
Inter-OA	0.4 (<0.001)	0.409 (<0.001)	0.347 (<0.001)	0.663 (<0.001)	0.335 (<0.001)	
Intra-OA	RON	0.744 (0.0003)	0.589 (0.0047)	0.913 (<0.0001)	0.826 (<0.001)	0.652 (0.0018)
	JBB	0.642 (0.0019)	0.359 (0.0737)	0.465 (0.0249)	0.742 (0.0002)	0.559 (0.0054)
	JOA	0.826 (<0.001)	0.603 (0.0016)	0.901 (<0.001)	0.485 (0.0133)	0.862 (<0.001)
	HPL	0.819 (<0.001)	0.893 (<0.001)	0.348 (0.0935)	0.721 (0.0005)	0.551 (0.005)

pCLE, probe-based confocal laser endomicroscopy.

standardization of a pCLE AOI is useful for better evaluation of the number of gastric glands and potential identification of CAG.

Our pCLE-histology gland density correlation and pCLE morphometric gland analysis are not exempt from limitations. First, although we found that the median number of glands per patient decreased as CAG severity increased, as reported in previous studies [24, 26], a standardized pCLE AOI for gland counting remains undefined. The use of standardized histological analysis parameters, such as glands/mL [8] or glands/40X microscope field, would make defining an AOI possible [14]. Indeed, our study's pCLE images were obtained from the gastric body mucosa, limiting its applicability in those patients with atrophic gastric in the gastric antrum and pyloric gland region. Second, the definition of a larger or smaller pCLE gastric gland was based on measurements observed in the NAG cohort; however, it should be evaluated in a healthy cohort. Third, we quantified the inter-glandular distance on pCLE only between adjacent glands to obtain the most objective measurement; thus, this approach is useful for analyzing adjacent glands but not meas-

uring larger inter-glandular distances after atrophic glands disappear [28]. Our study is also limited by several methodological aspects, such as lack of randomization and external validation, mainly due to this pilot study design; these limitations will be addressed in upcoming trials, mainly evaluating our proposed CAG criteria in other areas of the gastric mucosa such as antrum and pyloric gland region. Endoscopists should also consider that CAG and intestinal metaplasia distribution across the gastric body mucosa differs. Therefore, defining the AOI before evaluating with pCLE may influence the diagnostic and histological outcomes.

Nevertheless, our proposed criteria allow us to detect CAG in real time, avoiding misinterpretations when defining CAG and disagreements between observers. Furthermore, this may be one of the first studies aimed at measuring gastric gland area on pCLE and correlating it with CAG presence. Finally, our proposed pCLE criteria were designed to be applicable in daily practice and demonstrated reproducibility based on a moderate interobserver and excellent intra-observer agreement assessment.

Our proposed criteria indirectly measure gland size in the pCLE field using a visual approach. A systematic method that can accomplish this with the software will further improve the objectivity of these criteria and their reproducibility. In addition, the proposed criteria were driven by quantitative analysis of pCLE and histological evaluation of patients with CAG; the criteria require the evaluation and interpretation of an endoscopist. Nevertheless, novel artificial intelligence-based models may be able to apply these proposed criteria for real-time pCLE diagnosis of CAG in the future.

Conclusions

In conclusion, in our pilot study, the proposed pCLE criteria for CAG, based on gland density, size, and inter-glandular distance, had a good correlation with gland density determined with pCLE and histology. Our proposed CAG criteria are a reliable method with moderate interobserver and excellent intra-observer agreement; however, further studies with more pCLE image measurements are needed to confirm, adjust, and simplify the proposed criteria.

Competing interests

Dr. Robles-Medranda is a key opinion leader and consultant for Pentax Medical, Boston Scientific, G-tech Medical Supply, and MD Consulting Group.

References

- [1] Pimentel-Nunes P, Libânio D, Marcos-Pinto R et al. Management of epithelial precancerous conditions and lesions in the stomach (MAPS II): European Society of Gastrointestinal Endoscopy (ESGE), European Helicobacter and Microbiota Study Group (EHMSG), European Society of Pathology (ESP), and Sociedade Port. Endoscopy 2019; 51: 365–388
- [2] Weck MN, Brenner H. Prevalence of chronic atrophic gastritis in different parts of the world. Cancer Epidemiol Biomarkers Prev 2006; 15: 1083–1094
- [3] Song H, Ekhedden IG, Zheng Z et al. Incidence of gastric cancer among patients with gastric precancerous lesions: observational cohort study in a low risk Western population. BMJ 2015; 351: h3867 doi:10.1136/bmj.h3867
- [4] Kaji K, Hashiba A, Uotani C et al. Grading of atrophic gastritis is useful for risk stratification in endoscopic screening for gastric cancer. Am J Gastroenterol 2019; 1145: 71–79
- [5] Deutsch JC. The optical biopsy of small gastric lesions. Gastrointest Endosc 2014; 79: 64–65
- [6] Eshmuratov A, Nah JC, Kim N et al. The correlation of endoscopic and histological diagnosis of gastric atrophy. Dig Dis Sci 2010; 55: 1364–1375
- [7] Dixon MF, Genta RM, Yardley JH et al. Classification and grading of Gastritis: The updated Sydney system. Am J Surg Pathol 1996; 20: 1161–1181
- [8] Takechi K, Ohashi M, Koda K et al. Gastric pit density and depth of foveolae of the gastric body mucosa assessed by dye endoscopy. Dig Endosc 1993; 5: 231–237
- [9] Kodama M, Kodama T, Suzuki H et al. Effect of rice and salty rice diets on the structure of mouse stomach. Nutr Cancer 1985; 6: 135–147
- [10] Crafa P, Russo M, Miraglia C et al. From Sidney to OLGA: an overview of atrophic gastritis. Acta Biomed 2018; 89: 93–99
- [11] Andrew A, Wyatt J, Dixon M. Observer variation in the assessment of chronic gastritis according to the Sydney system. Histopathology 1994; 25: 317–322
- [12] Aydin O, Egilmez R, Karabacak T et al. Interobserver variation in histopathological assessment of *Helicobacter pylori* gastritis. World J Gastroenterol 2003; 9: 2232–2235
- [13] Staibano S, Rocco A, Mezza E et al. Diagnosis of chronic atrophic gastritis by morphometric image analysis. A new method to overcome the confounding effect of the inflammatory infiltrate. J Pathol 2002; 198: 47–54
- [14] Ruiz B, Garay J, Johnson W et al. Morphometric assessment of gastric antral atrophy: Comparison with visual evaluation. Histopathology 2001; 39: 235–242
- [15] Liu T, Zheng H, Gong W et al. The accuracy of confocal laser endomicroscopy, narrow band imaging, and chromoendoscopy for the detection of atrophic gastritis. J Clin Gastroenterol 2015; 49: 379–386
- [16] Robles-Medranda C, Vargas M, Ospina J et al. Clinical impact of confocal laser endomicroscopy in the management of gastrointestinal lesions with an uncertain diagnosis. World J Gastrointest Endosc 2017; 9: 389
- [17] Zhang JN, Li YQ, Zhao YA et al. Classification of gastric pit patterns by confocal endomicroscopy. Gastrointest Endosc 2008; 67: 843–853
- [18] Lancaster GA, Thabane L. Guidelines for reporting non-randomised pilot and feasibility studies. Pilot Feasibility Stud 2019; 5: 114
- [19] Rotondi MA, Donner A. A confidence interval approach to sample size estimation for interobserver agreement studies with multiple raters and outcomes. J Clin Epidemiol 2012; 65: 778–784
- [20] Minalyan A, Benhammou JN, Artashesyan A et al. Autoimmune atrophic gastritis. Clin Exp Gastroenterol 2017; 10: 19–27
- [21] Rugge M, Correa P, Dixon MF et al. Gastric mucosal atrophy: Interobserver consistency using new criteria for classification and grading. Aliment Pharmacol Ther 2002; 16: 1249–1259
- [22] Odze RD, Goldblum JR. Surgical pathology of the GI tract, liver, biliary tract and pancreas. SElsevier Inc 2009: doi:10.1016/B978-1-4160-4059-0.X5001-2
- [23] Lee SK. Usefulness and future prospects of confocal laser endomicroscopy for gastric premalignant and malignant lesions. Clin Endosc 2015; 48: 511–515
- [24] Wang P, Ji R, Yu T et al. Classification of histological severity of *Helicobacter pylori* – associated gastritis by confocal laser endomicroscopy. World J Gastroenterol 2010; 16: 5203–5210
- [25] Guamán-Guamán MI, Abarca-Ruiz JW. Validación endoscópica de la cromoespectroscopia virtual (FICE) en la detección de lesiones preneoplásicas gástricas vs histopatología. Universidad Central del Ecuador; 2018
- [26] Yu X, Chen J, Zheng L et al. Quantitative diagnosis of atrophic gastritis by probe-based confocal laser endomicroscopy. Biomed Res Int 2020; 2020: doi:10.1155/2020/9847591
- [27] Nguyen DL, Lee JG, Parekh NK et al. The current and future role of endomicroscopy in the management of inflammatory bowel disease. Ann Gastroenterol 2015; 28: 329–334
- [28] Genta RM. Gastric atrophy and atrophic gastritis - nebulous concepts in search of a definition. Aliment Pharmacol Ther 1998; 12: 17–23